Nociceptive Laser-Evoked Brain Potentials Do Not Reflect Nociceptive-Specific Neural Activity

A. Mouraux and G. D. Iannetti

J Neurophysiol 101:3258-3269, 2009. First published 1 April 2009; doi:10.1152/jn.91181.2008

Journal of Neurophysiology publishes original articles on the function of the nervous system. It is published 12 times a year (monthly) by the American Physiological Society, 9650 Rockville Pike, Bethesda MD 20814-3991. ISSN: 0022-3077, ESSN: 1522-1598. Visit our website at http://www.the-aps.org/.

J Neurophysiol 101: 3258–3269, 2009.
First published April 1, 2009; doi:10.1152/jn.91181.2008.

Nociceptive Laser-Evoked Brain Potentials Do Not Reflect Nociceptive-Specific Neural Activity

A. Mouraux[1] and G. D. Iannetti[2]

[1]*Departments of Clinical Neurology and* [2]*Physiology, Anatomy, and Genetics, University of Oxford, Oxford, United Kingdom*

Submitted 2 November 2008; accepted in final form 27 March 2009

Mouraux A, Iannetti GD. Nociceptive laser-evoked brain potentials do not reflect nociceptive-specific neural activity. *J Neurophysiol* 101: 3258–3269, 2009. First published April 1, 2009; doi:10.1152/jn.91181.2008. Brief radiant laser pulses can be used to activate cutaneous Aδ and C nociceptors selectively and elicit a number of transient brain responses [laser-evoked potentials (LEPs)] in the ongoing EEG. LEPs have been used extensively in the past 30 years to gain knowledge about the cortical mechanisms underlying nociception and pain in humans, by assuming that they reflect at least neural activities uniquely or preferentially involved in processing nociceptive input. Here, by applying a novel blind source separation algorithm (probabilistic independent component analysis) to 124-channel event-related potentials elicited by a random sequence of nociceptive and non-nociceptive somatosensory, auditory, and visual stimuli, we provide compelling evidence that this assumption is incorrect: LEPs do not reflect nociceptive-specific neural activity. Indeed, our results indicate that LEPs can be entirely explained by a combination of multimodal neural activities (i.e., activities also elicited by stimuli of other sensory modalities) and somatosensory-specific, but not nociceptive-specific, neural activities (i.e., activities elicited by both nociceptive and non-nociceptive somatosensory stimuli). Regardless of the sensory modality of the eliciting stimulus, the magnitude of multimodal activities correlated with the subjective rating of saliency, suggesting that these multimodal activities are involved in stimulus-triggered mechanisms of arousal or attentional reorientation.

INTRODUCTION

How does the brain process nociceptive input, and how does this processing lead to the perception of pain? Human electrophysiological studies using EEG, magnetoencephalography (MEG), or invasive intra-cerebral recordings, as well as hemodynamic studies using functional MRI (fMRI) or positron emission tomography (PET), have all emphasized the fact that nociceptive stimuli elicit consistent responses in a large array of cortical structures (Bushnell and Apkarian 2005; Garcia-Larrea et al. 2003; Kakigi et al. 2005; Peyron et al. 2000, 2002; Treede et al. 1999), including primary and secondary somatosensory cortices (SI and SII), the insula, and the anterior cingulate cortex (ACC). Although several investigators have suggested that these responses could be largely unspecific for pain (Bromm and Lorenz 1998; Carmon et al. 1976; Garcia-Larrea et al. 1997; Iannetti et al. 2008; Kunde and Treede 1993; Mouraux and Plaghki 2006; Peyron et al. 2000; Stowell 1984), this assembly of cortical structures, often referred to as the "pain matrix," has been repeatedly interpreted as forming a network uniquely or preferentially involved in the perception of pain (Boly et al. 2008; Brooks and Tracey 2005; Cheng et al. 2007; Costantini et al. 2008; Decety et al. 2008; Ducreux et al. 2006; Ingvar 1999; Jones 1998a; Maihofner et al. 2007; Moisset and Bouhassira 2007; Singer et al. 2004; Stern et al. 2006; Valeriani et al. 2008; Whyte 2008). In support of the "pain-specific" interpretation of these responses, two common experimental findings are often brought forward. First, in most experimental settings, the magnitude of activity in the "pain matrix" correlates robustly with the intensity of perceived pain (Coghill et al. 1999; Derbyshire et al. 1997; Iannetti et al. 2005), a finding interpreted as indicating that at least part of the "pain matrix" reflects "neural mechanisms for pain intensity coding in the human cortex" (Porro 2003). Second, the top-down cognitive modulation of specific aspects of pain perception can selectively alter the response magnitude in specific subregions of the "pain matrix" (e.g., hypnotic modulation of the intensity of perceived pain could specifically change the response magnitude in SI, whereas hypnotic modulation of the unpleasantness of perceived pain could specifically change the response magnitude in the ACC; Hofbauer et al. 2001; Rainville et al. 1997), a finding often interpreted as indicating that these subregions serve different functions related to the perception of pain.

Brief radiant laser pulses, by activating cutaneous Aδ and C nociceptors selectively, provide a purely nociceptive input and elicit, in the ongoing EEG, a number of transient brain responses (Carmon et al. 1976), related to the activation of Aδ skin nociceptors (Treede et al. 1995). The larger part of the laser-evoked potential (LEP) response is represented by a negative-positive biphasic wave (N2-P2), peaking ~200–350 ms after hand stimulation, and maximal at the scalp vertex (Bromm and Treede 1987). This N2–P2 complex is preceded by an earlier response, the N1 wave, peaking at ~160 ms, and maximal over the temporal region contralateral to the stimulated side (Treede et al. 1988). Source analysis studies have shown that LEPs can be modeled by a combination of generators located within the so-called "pain matrix" (i.e., SI, SII, the insula, and the ACC; reviewed in Garcia-Larrea et al. 2003), and results obtained from subdural (Lenz et al. 1998a,b; Ohara et al. 2004) and intracerebral (Frot and Mauguiere 2003; Frot et al. 1999, 2008) recordings in humans have confirmed that nociceptive stimuli elicit responses within these regions.

However, as already pointed-out by Carmon et al. (1976) in their seminal work, as well as by Stowell (1984), the fact that the eliciting sensory stimulus is entirely selective for nociceptive peripheral afferents by no means implies that the elicited brain activity is nociceptive specific. As a matter of fact, non-nociceptive somatosensory stimuli (Garcia-Larrea et al. 1995; Goff et al. 1977), auditory stimuli (Naatanen and Picton 1987; Picton et al. 1999), and even visual stimuli (Makeig et al. 1999; Vogel and Luck 2000) may all elicit a large "vertex potential" whose shape, scalp topography, and sensitivity to

Address for reprint requests and other correspondence: G. Iannetti, Dept. of Physiology, Anatomy, and Genetics, Univ. of Oxford, South Parks Rd., OX1 3QX Oxford, UK (E-mail: giandomenico.iannetti@dpag.ox.ac.uk).

various experimental factors closely resemble those of LEPs (Garcia-Larrea 2004; Garcia-Larrea et al. 2003; Kunde and Treede 1993; Mouraux and Plaghki 2006). Furthermore, we recently showed that laser stimuli perceived as more painful could elicit LEPs of greater magnitude simply because they are more salient (Iannetti et al. 2008). In support of this interpretation, Legrain et al. (2003, 2005) showed that at least part of the activity underlying LEPs is likely to reflect involuntary mechanism of attentional reorientation rather than nociceptive processing per se (see also Lorenz and Garcia-Larrea 2003 for a review). Taken together, these experimental observations question the appropriateness of assuming that LEPs reflect neuronal activities uniquely or even preferentially involved in processing nociceptive input.

Therefore to test the validity of the assumption that LEPs reflect neuronal activities uniquely or preferentially involved in processing nociceptive input, we applied a novel blind source separation algorithm probabilistic independent component analysis (PICA) (Beckmann and Smith 2004; Makeig et al. 1997), to event-related potentials (ERPs) recorded using high-density scalp EEG (124 channels). By comparing the ERPs elicited by a random sequence of nociceptive and non-nociceptive somatosensory stimuli, auditory stimuli, and visual stimuli, we quantified and characterized, at single-subject level, the respective contribution of multimodal neural activities (i.e., activities also elicited by stimuli of other sensory modalities), somatosensory-specific neural activities (i.e., activities elicited by both nociceptive and non-nociceptive somatosensory stimuli), and nociceptive-specific neural activities (i.e., activities uniquely elicited by nociceptive somatosensory stimuli) to the LEP response.

METHODS

Ethical approval

The study conformed to the latest revision of the Declaration of Helsinki. All experimental procedures were approved by the Oxfordshire Research Ethics Committee. Written informed consent was obtained from all participants.

Participants

Nine healthy right-handed volunteers (4 females and 5 males; age, 20–32 yr) participated in the study. Before the electrophysiological recording, the experimental setup and the psychophysical rating task were clearly explained to the participants, who were also exposed to a small number of test stimuli (5–10 stimuli for each stimulus type).

Experimental design

Experiments were conducted in a dim, silent, temperature-controlled room. Participants lay semi-supine in a comfortable armchair while receiving brief stimuli belonging to four different sensory modalities: nociceptive somatosensory, non-nociceptive somatosensory, auditory, and visual. Participants were instructed to keep their gaze fixed on a white cross (3 × 3 cm) placed centrally in front of them, at a distance of ~2 m, 30° below eye level. To ensure that observed differences in the recorded responses were not related to the spatial location of the stimulus or to spatial attention (two experimental factors that have been shown to influence the magnitude and scalp topography of ERPs; e.g., Legrain et al. 2002; Schlereth et al. 2003), all sensory stimuli were delivered in a random sequence to or near the dorsum of the right hand (Fig. 1, *top left*), which was placed ~45 cm from the participant's head, 25° right of the midline, and 30° below eye level. The experiment was divided in four successive runs. The number of trials for each run ranged between 38 and 42, and each type

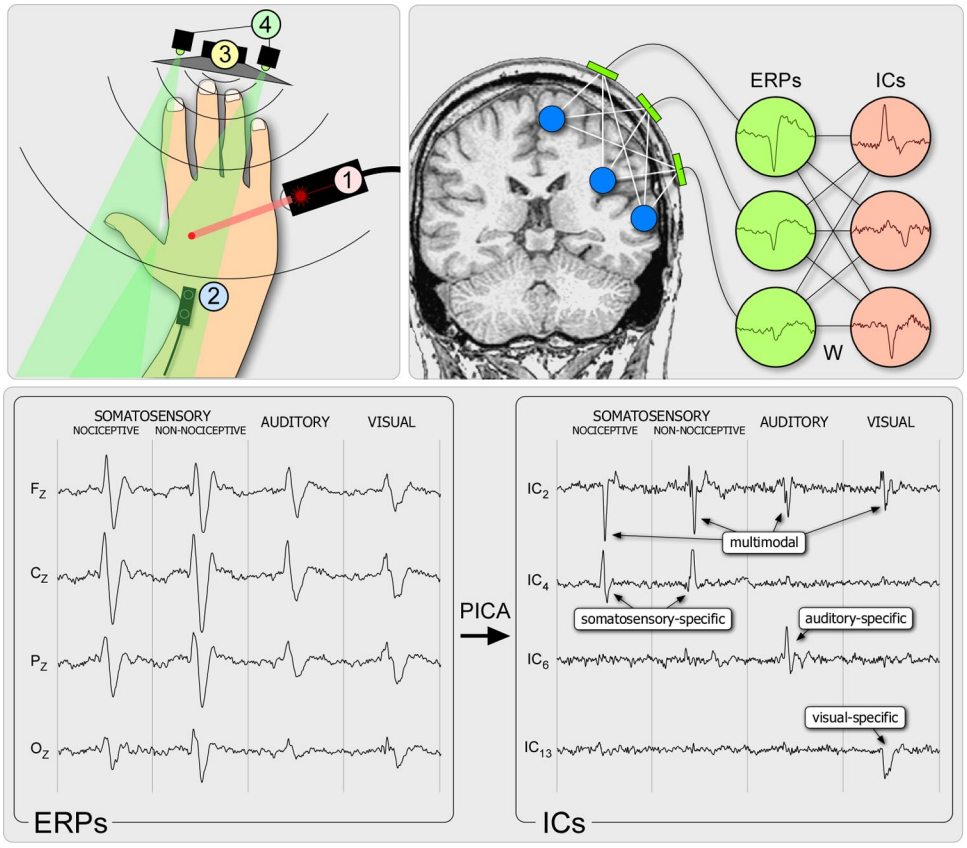

FIG. 1. Experimental procedure. 124-channel event-related potentials (ERPs) were elicited by a random sequence of nociceptive and non-nociceptive somatosensory, auditory, and visual stimuli. *Top left*: all stimuli were delivered to or near the right hand dorsum. Nociceptive somatosensory stimuli (*1*) were brief infrared laser pulses delivered to the sensory territory of the superficial radial nerve; non-nociceptive somatosensory stimuli (*2*) were brief electrical pulses applied to the same nerve; auditory stimuli (*3*) were brief tones produced by a speaker; visual stimuli (*4*) were brief flashes produced by 2 light-emitting diodes. *Top right*: scalp electrodes record a linear mixture of the activity produced by a number of spatially distinct neural generators. Probabilistic independent component analysis (PICA) was used to optimize a matrix (*W*) that unmixed scalp ERPs into a set of temporally independent and spatially fixed independent components (ICs). *Bottom*: when applied to the 4 ERPs concatenated into a single waveform, PICA separated effectively modality-specific from multimodal activities. Note how, because of volume conduction, ERPs spread across the 4 representative electrodes shown in the *bottom left panel*. Also note the clear temporal independence of the 4 representative ICs shown in the *bottom right panel*. IC 2 contributed to all 4 ERPs and was categorized as multimodal. ICs 4, 6, and 13 contributed uniquely to the ERP elicited by one or a subset of stimuli and were respectively categorized as somatosensory, auditory, and visual specific.

of stimulus was similarly represented in each run. In total, each type of stimulus was delivered 40 times. Interstimulus interval was 5–10 s (random square distribution). To ensure that vigilance was maintained across time, and that each type of sensory stimulus was equally relevant to the task, participants were instructed to report the total number of perceived stimuli at the end of each of the four runs. Finally, at the end of the experiment, participants were asked to rate the saliency of each type of stimulus using a numerical scale ranging from 0 (not salient) to 10 (extremely salient). Stimulus saliency was explained to each subject as "the ability of the stimulus to capture attention." Therefore it was expected to integrate several factors such as stimulus intensity, frequency of appearance, novelty, and its potential relevance to behavior. Several studies have shown that human judgments of saliency correlate well with predicted models of saliency (Kayser et al. 2005).

Sensory stimuli

Nociceptive somatosensory stimuli were pulses of radiant heat (4-ms duration) generated by an infrared neodymium yttrium aluminum perovskite (Nd:YAP) laser (wavelength: 1.34 μm; ElEn Group). Stimulus target was the sensory territory of the superficial radial nerve. Beam diameter at the target site was ~7 mm. For each participant, stimulus energy (2.3 ± 0.3 J) was adjusted to elicit a clear painful pinprick sensation related to the activation of Aδ skin nociceptors (Bromm and Treede 1984; Iannetti et al. 2006). To prevent nociceptor fatigue or sensitization, the laser target was displaced after each pulse. Non-nociceptive somatosensory stimuli were constant current square-wave electrical pulses (1-ms duration; DS7A, Digitimer) delivered through a pair of skin electrodes (0.5 cm diam, 1-cm interelectrode distance) placed at the wrist, over the superficial radial nerve. For each participant, stimulus intensity (9.9 ± 2.1 mA) was adjusted to elicit a nonpainful paresthesia in the corresponding sensory territory. This intensity of electrical stimulation was above the threshold of Aβ fibers (which convey non-nociceptive tactile information) but below the threshold of nociceptive Aδ and C fibers (Burgess and Perl 1967; also see RESULTS). Auditory stimuli were brief 800-Hz tones (50-ms duration; 5-ms rise and fall times) presented at a loud but comfortable listening level (~85 dB SPL) and delivered through a speaker (VE100AO, Audax) placed in front of the participant's hand. Visual stimuli were brief flashes (5-ms duration) delivered by two green light-emitting diodes (11.6 cd, 15° viewing angle) pointing toward the participants head, and placed on top of the speaker.

Electrophysiological recording

The EEG was recorded using 124 Ag-AgCl electrodes placed on the scalp according to the International 10–5 system and referenced to the nose. Ocular movements and eye blinks were recorded using two surface electrodes placed at the top left and bottom right sides of the right eye. In addition, the ECG was recorded using two surface electrodes placed at the left and right wrists. Signals were amplified and digitized using a sampling rate of 1,024 Hz (SD128 EEG, Micromed). Continuous EEG recordings were segmented into 1.5-s epochs (−0.5 to +1.0 s relative to stimulus onset) and band-pass filtered (1–30 Hz). After baseline correction (reference interval −0.5 to 0 s), artifacts produced by eye blinks or eye movements were subtracted using a validated method (Jung et al. 2000) based on an independent component analysis (ICA). In addition, epochs with amplitude values exceeding ±100 μV (i.e., epochs likely to be contaminated by an artifact) were rejected. These epochs constituted 5 ± 3% of the total number of epochs. Separate average ERP waveforms were computed for each participant and stimulus type (nociceptive somatosensory, non-nociceptive somatosensory, auditory, and visual). All EEG processing steps were carried out using Letswave (amouraux.webnode.com/letswave; Mouraux and Iannetti 2008), Matlab (The MathWorks), and EEGLAB (sccn.ucsd.edu/eeglab; Delorme and Makeig 2004).

Blind source separation using PICA

For each subject, multimodal and modality-specific neural activities were separated using an ICA (Makeig et al. 1997) constrained to an effective estimate of the intrinsic dimensionality of the original data (PICA; Beckmann and Smith 2004). When applied to multi-channel EEG recordings (Fig. 1, *top right*), ICA separates the signals recorded on the scalp into a linear combination of independent components (ICs), each having a fixed scalp topography and a maximally independent time course. When ICA is unconstrained, the total number of estimated ICs equals the total number of recording electrodes. If the number of estimated ICs differs greatly from the actual number of independent sources contributing to the signal, this may constitute a critical problem (Beckmann and Smith 2004). Indeed, if the number of estimated ICs is much larger than the number of sources, ICs containing spurious activity will appear because of overfitting. On the contrary, if the number of estimated ICs is much smaller than the number of sources, valuable information will be lost because of underfitting. This fundamental limitation can be addressed using PICA, a method that constrains the total number of estimated ICs to an effective estimate of the number of independent sources contributing to the original data and that was initially developed for the analysis of fMRI signals (Beckmann and Smith 2004). As a result, each obtained IC is more likely to represent a single physiological source of activity.

For each participant, the ERPs elicited by nociceptive somatosensory, non-nociceptive somatosensory, auditory, and visual stimuli were concatenated into a single waveform (4 average waveforms × 1.5 s × 1,024 Hz = 6,144 time points; Fig. 1, *bottom left*). To constrain ICA, an objective estimate of the number of independent sources contributing to the four ERP waveforms was obtained using a method based on maximum likelihoods and operating on the eigenvalues of a principal component analysis (Rajan and Rayner 1997). The blind source separation was performed on the concatenated waveform using runica (Delorme and Makeig 2004; Makeig et al. 1997), an automated form of the extended infomax ICA algorithm (Bell and Sejnowski 1995), constrained to the estimated number of dimensions (Fig. 1, *bottom*).

We assumed that nociceptive somatosensory LEPs, such as non-nociceptive somatosensory ERPs (SEPs), auditory ERPs (AEPs), and visual ERPs (VEPs), resulted from a linear mixture of multimodal and modality-specific cortical activities projected onto the scalp, each having distinct yet possibly overlapping time courses. Although multimodal activities would contribute to all four segments of the concatenated ERP waveform, modality-specific activities would contribute only to the segment corresponding to the ERP elicited by stimuli belonging to a particular sensory modality (e.g., auditory-specific activity would contribute to the AEP segment of the concatenated ERP time course, but not to the LEP, the SEP, or the VEP segments of that same concatenated ERP time course). Therefore, because multimodal and modality-specific activities would contribute differently to each of the four segments of the concatenated ERP time course, we hypothesized that PICA would be able to separate these activities into distinct ICs, provided that they had nonidentical scalp topographies. It is worth noting that this procedure did not require that the time course of multimodal neural activity be identical across sensory modalities. This is important because the time course of multimodal neural activity may be expected to differ because of various physiological reasons (e.g., the different transduction mechanisms and conduction velocities of activated primary afferents).

To estimate the contribution of each obtained IC to the ERP elicited in each of the four explored sensory modalities, the time course of the power of each IC (μV^2) was expressed as the SD from the mean (z-scores) of the concatenated prestimulus intervals of all four average

waveforms (−0.5 to 0 s). z-scores were averaged within the 0 to +0.5 s interval following the onset of each stimulus, thus yielding four values for each IC (1 value for each stimulus type). If at least one of these four values was greater than $z = 1.5$, the IC was considered to reflect stimulus-evoked activity. These ICs were categorized according to their relative contribution to the four ERPs. For each IC and stimulus type, we computed the ratios between the signal power contributed to the ERP elicited by that stimulus type and the signal power contributed to the ERPs elicited by each of the three other stimulus types. If the ratio was ≥3.5 for one stimulus type versus each of the other three stimulus types (i.e., the IC contributed uniquely to one of the four ERP segments), the IC was categorized as modality specific (nociceptive somatosensory, non-nociceptive somatosensory, auditory, or visual). Furthermore, if the calculated ratio for that IC was ≥3.5 for both the LEP and the SEP versus the AEP and the VEP (i.e., the IC contributed to the LEP and the SEP but not to the AEP and the VEP), it was categorized as somatosensory specific. Remaining ICs (i.e., ICs that contributed to all four ERP segments) were categorized as multimodal. Figure 2 shows how this method allowed breaking down effectively LEPs, SEPs, AEPs, and VEPs into a set of multimodal and modality-specific components. It is important to highlight that the obtained classification was not critically dependent on the arbitrarily defined threshold of 3.5 (which was chosen because it matched well the decision of 2 blinded observers). Indeed, most ICs were unambiguously multimodal or modality-specific, and IC classifications obtained using different cut-off values ranging between 2 and 4.5 yielded results that were not noticeably different from those obtained using a cut-off of 3.5 (data not shown).

RESULTS

Psychophysical results

Subjects reliably reported the number of stimuli presented in each run, with an average error rate of 1 ± 2 (SD).

All subjects described the sensation elicited by the laser stimulus as painful and clearly pricking. However, compared with the other three stimulus types, the laser stimulus was not systematically reported as the most salient (Fig. 7, *left*). In fact, the average ratings for stimulus saliency (nociceptive somatosensory stimuli: 6.1 ± 1.6, non-nociceptive somatosensory stimuli: 5.3 ± 1.2, auditory stimuli: 5.5 ± 1.7, visual stimuli: 4.3 ± 1.7) were not significantly different across stimulus types (repeated-measures ANOVA, $P = 0.12$).

ERP waveforms and topographies

LEPs consisted of a large negative-positive biphasic wave (N2–P2) that was maximal over the scalp vertex (electrode Cz; Fig. 2, *top row*). Whereas the laser-evoked N2 extended bilaterally toward temporal regions (electrodes T3 and T4), the laser-evoked P2 was more centrally distributed. Preceding the laser-evoked N2, and often appearing within its ascending shoulder, the laser-evoked N1 was maximal over the temporal area contralateral to the stimulated side (electrode T3; Fig. 3).

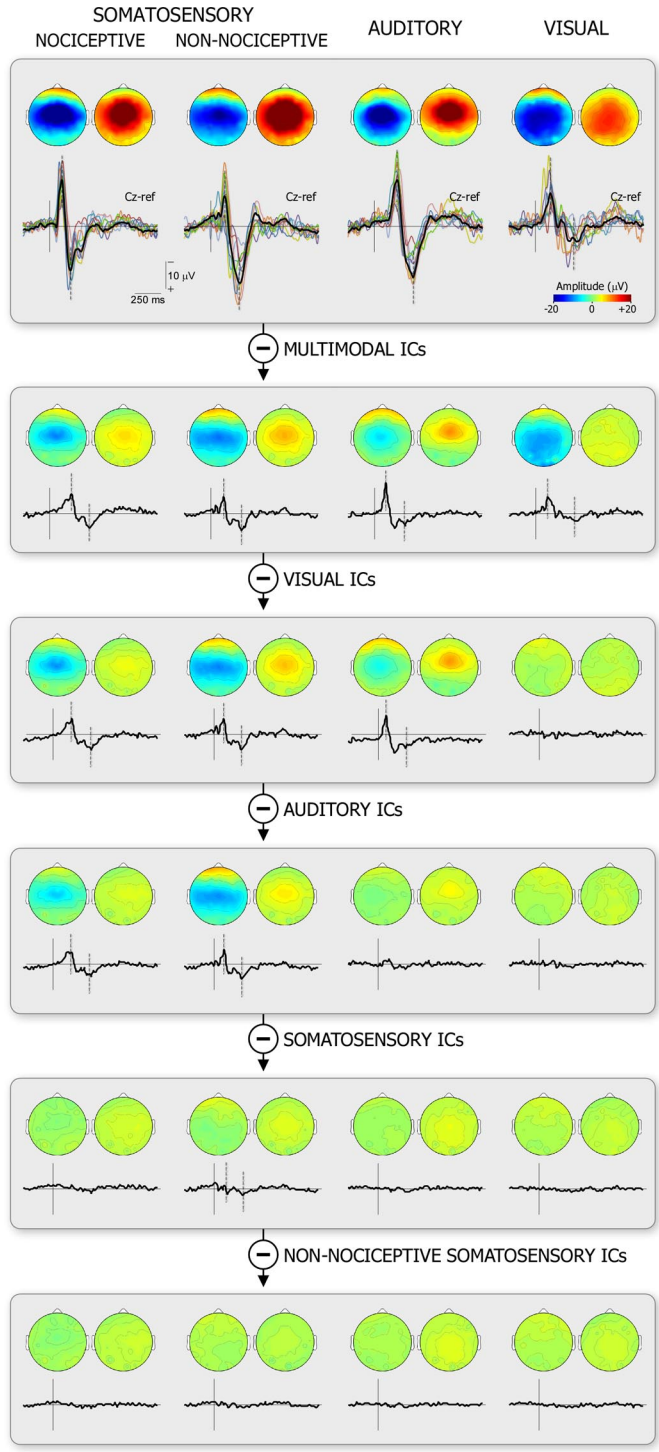

FIG. 2. Contribution of multimodal and modality-specific activities to sensory ERPs. *First row*: for each stimulus type, the colored waveforms correspond to single-subject ERPs, whereas the black waveform corresponds to the group average (electrode Cz vs. nose reference). Vertical lines mark the stimulus onset. Whatever the sensory modality of the eliciting stimulus, the greater part of the ERP consisted of a large negative-positive biphasic wave whose shape and scalp topography were remarkably similar. PICA was used to break down these ERPs into a set of multimodal and modality-specific ICs. *Second row*: ERP waveforms obtained after subtracting ICs categorized as multimodal. Note how this subtraction markedly reduces signal amplitude, thus showing that multimodal brain responses are the main constituent of all four ERP waveforms. *Following rows*: ERP waveforms obtained after sequentially subtracting visual (*3rd row*), auditory (*4th row*), somatosensory (*5th row*), and non-nociceptive somatosensory (*6th row*) ICs. After the removal of each category of modality-specific ICs, the amplitude of the ERP elicited by the stimulus belonging to that sensory modality tends toward 0, whereas the ERP elicited by stimuli belonging to other sensory modalities is largely unaffected. Note that somatosensory ICs contribute to both the nociceptive and the non-nociceptive somatosensory ERP, whereas non-nociceptive somatosensory ICs contribute uniquely to the non-nociceptive somatosensory ERP. Also note the absence of nociceptive somatosensory ICs. All waveforms and scalp maps are shown using the same scale.

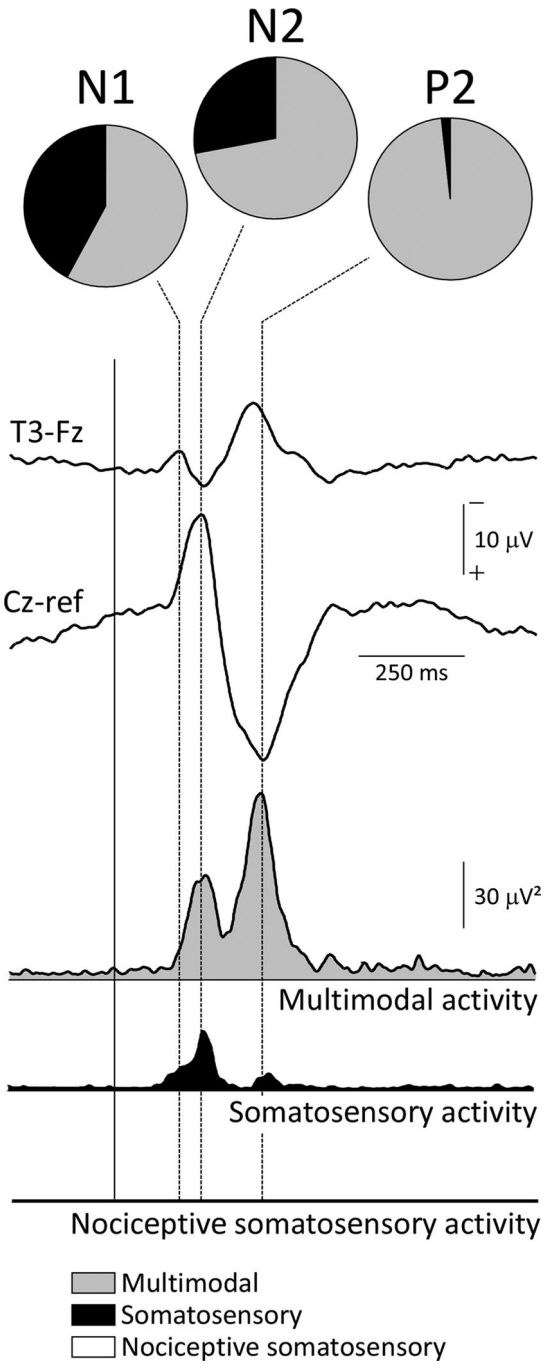

FIG. 3. Multimodal and somatosensory-specific activities contributing to the laser-evoked potential (LEP) waveform. LEPs appear as a large negative-positive biphasic wave (N2–P2), maximal at the scalp vertex (shown here at Cz vs. nose reference; group average). An earlier negative wave (N1) precedes the N2-P2 complex. The N1 is maximal over the temporal area contralateral to the stimulated side (shown here at T3 vs. Fz). The greater part of the LEP waveform is explained by multimodal brain activity (i.e., activity also elicited by stimuli of other sensory modalities). The time course of this multimodal activity, expressed as global field power (μV^2), is shown in gray. Note how multimodal activity explains the greater part of the N1 and N2 waves and almost all of the P2 wave. Somatosensory-specific brain activity (i.e., activity elicited by both nociceptive and non-nociceptive somatosensory stimuli) also contributes to the LEP waveform. The time course of somatosensory-specific activity, expressed as global field power (μV^2), is shown in black. Note how its contribution is largely confined to the time interval corresponding to the N1 and N2 waves. Also note the lack of nociceptive-specific somatosensory activity contributing to the LEP.

Non-nociceptive somatosensory stimuli (N1–P2), auditory stimuli (N1–P2), and visual stimuli (N1–P3) elicited a negative-positive biphasic wave whose shape and scalp topography were similar to that of the LEP (Fig. 2, *top row*). The scalp topography of the laser-evoked N2 was indistinguishable from the scalp topography of the non-nociceptive somatosensory N1, both waves being maximal at the vertex and extending bilaterally over temporal regions. Furthermore, the initial part of the non-nociceptive somatosensory N1 was, such as the laser-evoked N1, greater over the hemisphere contralateral to the stimulated side. The scalp topography of the laser-evoked N2 also resembled closely that of the auditory N1, which extended bilaterally toward temporal regions, but was symmetrically distributed over both hemispheres. In contrast, the scalp topography of the laser-evoked N2 was not as markedly similar to the visual N1, which extended toward temporal and occipital areas, and clearly predominated over the hemisphere contralateral to the stimulated side.

The scalp topography of the laser-evoked P2 was indistinguishable from the scalp topography of the non-nociceptive somatosensory P2, the auditory P2, and the visual P3 (Fig. 2, *top row*). Indeed, whatever the sensory modality of the eliciting stimulus, this late positive wave was maximal over the vertex, and centrally distributed.

Peak latencies of the laser-evoked N2-P2 (199 ± 19 and 333 ± 25 ms), the non-nociceptive somatosensory N1-P2 (114 ± 28 and 251 ± 33 ms), the auditory N1-P2 (109 ± 14 and 211 ± 40 ms), and the visual N1-P3 (140 ± 15 and 333 ± 48 ms) were significantly different (negative peak: $P < 0.0001$; positive peak: $P < 0.0001$; repeated-measures ANOVA). These differences in peak latency can be largely explained by differences in the time required for the transduction of the stimulus energy into a neural impulse, as well as by differences in the time required for the sensory afferent volley to reach the cortex (peripheral and central conduction times). For example, the difference (~80 ms) between nociceptive and non-nociceptive somatosensory responses is explained by the difference between the conduction velocity of small-diameter nociceptive Aδ fibers (~10–15 m/s) and the conduction velocity of large-diameter non-nociceptive Aβ fibers (~50–100 m/s) (Inui et al. 2003).

Blind source separation of ERPs

The estimated number of independent sources contributing to the four ERP waveforms ranged, across participants, from 13 to 25 (20 ± 4). Constraining the ICA to this number of dimensions accounted for 99% of the variance of all four sensory ERPs; 15 ± 2 of these ICs were classified as contributing significantly to at least one of the four sensory ERPs and accounted for 96% of their variance. According to their relative contribution to LEP, SEP, AEP, and VEP segments of the concatenated ERP waveform, these ICs were categorized as either multimodal (Fig. 4) or modality-specific (Figs. 5 and 6).

Multimodal ICs

Multimodal neural activity (7 ± 3 ICs; Figs. 2 and 4) was the main constituent of all four sensory ERPs, explaining 76 ± 13% of the LEP waveform, 66 ± 17% of the SEP waveform, 62 ±

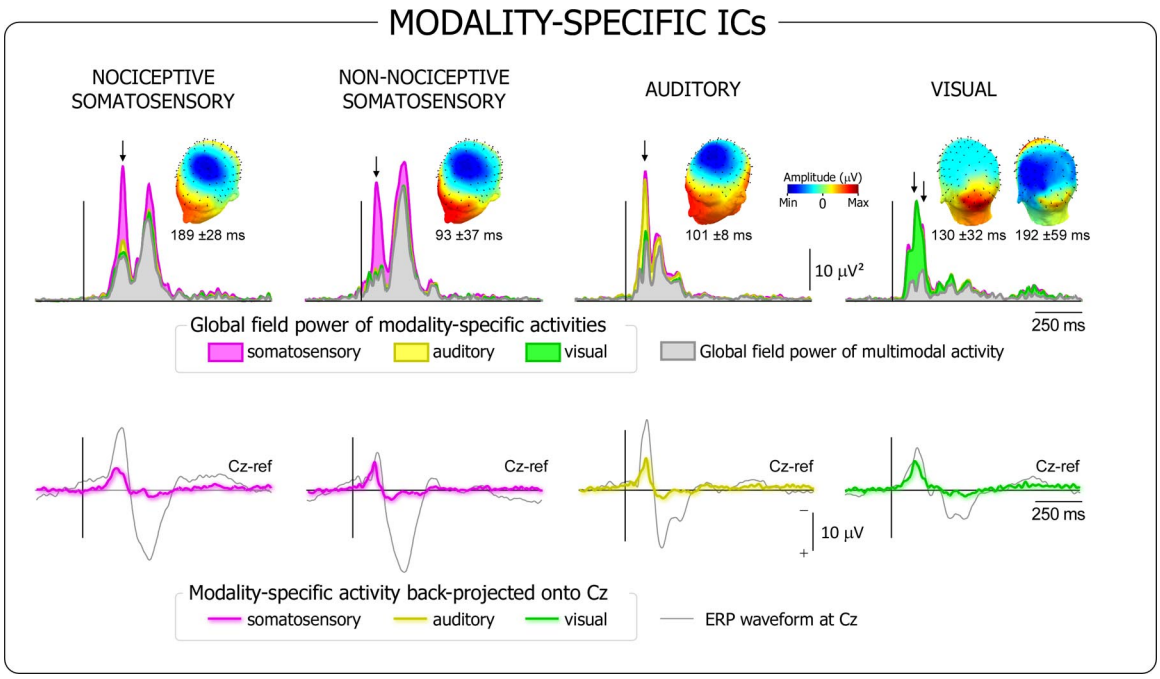

FIG. 4. Contribution of multimodal brain activity to sensory ERPs. PICA was used to break down ERPs of each participant into a set of multimodal and modality-specific ICs. *Left*: the spider chart shows the respective contribution of multimodal activity (expressed as the percentage of explained ERP variance) to the four sensory ERPs (represented on the four axes). Each colored line represents a single participant. Note how this multimodal activity contributes significantly to the four sensory ERPs in each participant. *Right*: the time course of multimodal activity, backprojected on the scalp and expressed as global field power (μV^2), is shown in the middle graphs (group average). Whatever the sensory modality of the eliciting stimulus, multimodal activity forms two peaks, whose scalp topographies are maximal at the vertex (top scalp maps). Note (bottom waveforms) how multimodal activity (thick line) explains the greater part of the ERP recorded at the scalp vertex (thin gray line).

25% of the AEP waveform, and 55 ± 26% of the VEP waveform. This multimodal activity consisted of a negative-positive biphasic wave, always maximal at the vertex (electrode Cz). The scalp topography of the negative peak extended bilaterally toward temporal regions, whereas the scalp topography of the positive peak was more centrally distributed. These topographies were very similar to those of the main negative (N2) and positive (P2) waves of the LEP. The latency of the negative and positive peaks of multimodal activity contributing to the LEP (200 ± 20 and 356 ± 47 ms), the SEP (109 ± 26 and 271 ± 38 ms), the AEP (109 ± 16 and 203 ± 34 ms), and the VEP (156 ± 38 and 330 ± 72 ms) closely matched the latencies of the corresponding negative and positive ERP peaks (Fig. 4).

CORRELATION BETWEEN THE MAGNITUDE OF MULTIMODAL ACTIVITY AND THE SUBJECTIVE RATING OF STIMULUS SALIENCY. For each participant and stimulus type, the magnitude of multimodal activity, expressed as the global field power (Lehmann and Skrandies 1980) of multimodal ICs backprojected onto the scalp and averaged within the 0 to 500 ms interval following stimulus onset, was plotted against the corresponding rating of stimulus saliency (Fig. 7, *left*). The linear dependence between these two variables was calculated for each subject using Pearson's correlation coefficient. Regardless of the sensory modality of the eliciting stimulus, the magnitude of multimodal activity was positively correlated with the subjective rating of stimulus saliency (Pearson's $r = 0.56 \pm 0.46$, group-level

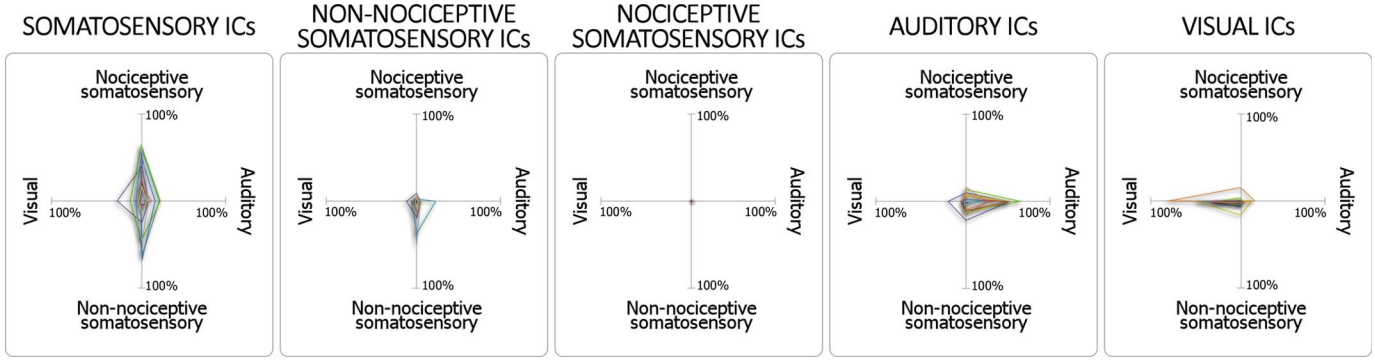

FIG. 5. Contribution of modality-specific brain activity to sensory ERPs. Spider charts show the respective contribution (expressed as the percentage of explained ERP variance) of somatosensory (*1st panel*), non-nociceptive somatosensory (*2nd panel*), nociceptive somatosensory (*3rd panel*), auditory (*4th panel*), and visual (*5th panel*) ICs to nociceptive and non-nociceptive somatosensory, auditory, and visual ERPs (represented on the four axes; each participant is shown as a colored line). Note how somatosensory ICs contribute to both nociceptive and non-nociceptive somatosensory ERPs, whereas non-nociceptive somatosensory, auditory and visual ICs contribute uniquely to the corresponding ERP waveforms. Also note the absence of nociceptive somatosensory ICs.

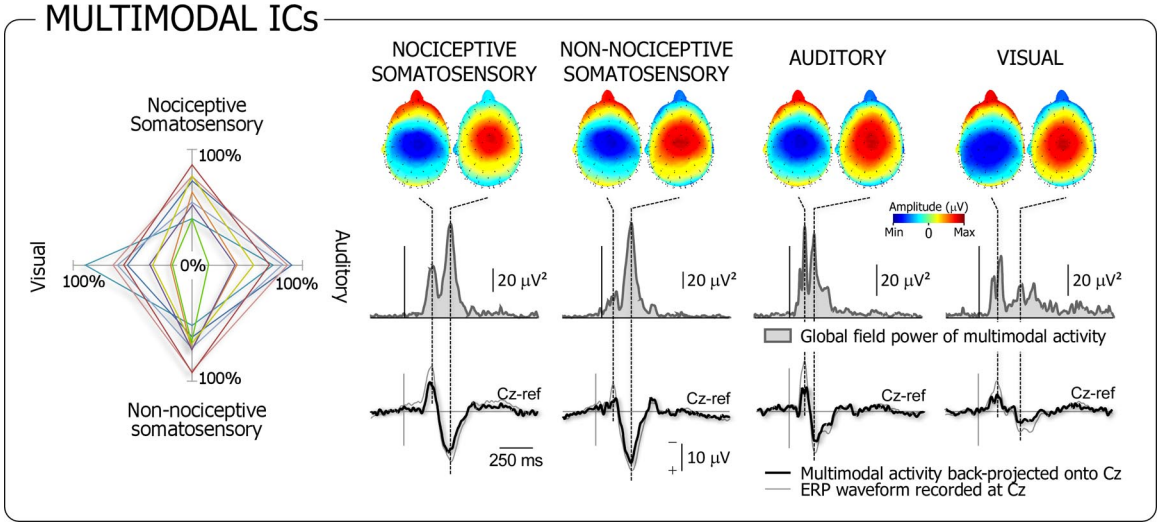

FIG. 6. Time course and scalp topography of modality-specific brain activity contributing to sensory ERPs. *Top row*: the group average time courses of multimodal (in gray) and modality-specific (in color) activities are shown in the cumulative stacked waveforms, backprojected on the scalp and expressed as the signal global field power (μV^2). *Bottom row*: average contribution of modality-specific brain activities (colored waveforms) to the ERP recorded from electrode Cz (thin gray waveform). Note how the contribution of somatosensory, auditory, and visual-specific activity is largely confined to the early part of the ERP time course. The scalp maps show the scalp topography of the main peaks of modality-specific brain activity. Somatosensory-specific activity appeared as a negative peak distributed over central and parietal regions, and maximal over the hemisphere contralateral to the stimulated side. Auditory-specific activity appeared as negative peak symmetrically distributed over central, frontal, and temporal regions. Visual-specific activity appeared as a positive peak followed by a negative peak, each peak showing a distinct scalp topography. The 1st peak of visual-specific activity was maximal over occipital areas. The 2nd was more largely distributed over parietal, temporal, and occipital areas and was maximal over the hemisphere contralateral to the stimulated side.

average). To examine the significance of this correlation across the group, single-subject correlation coefficients were normalized using Fisher's z transformation. The resulting z values were significantly different from zero ($t = 3.44$, $P = 0.009$).

SOURCE MODELING OF MULTIMODAL ICS. The location of the sources of multimodal ICs was modeled by fitting two symmetrical equivalent dipoles for each multimodal IC (7 ± 3 ICs for each subject). Dipole fitting was performed using an algorithm based on a nonlinear optimization technique and a standardized boundary element head model (*dipfit2*; Fuchs et al. 2002; Woody 1967). Dipole locations outside the head, and dipole models with a residual variance exceeding 20% were excluded. For each subject, 5 ± 2 multimodal ICs (accounting for 94% of the multimodal activity) were successfully modeled (average residual variance: 10.8 ± 6.4%). The locations of the fitted dipole pairs (Fig. 7, *right*) appeared to form two clusters: a deep midline cluster (-20 mm $< x <$20 mm, Montreal Neurological Institute coordinates) whose center of gravity was located in the ACC, and a bilateral cluster ($x < -20$ mm or $x >$20 mm) located in the left and right operculo-insular regions.

Modality-specific ICs

Modality-specific neural activities were identified in all participants, but their contribution to the recorded ERP waveforms was quantitatively smaller than the contribution of multimodal activity (Figs. 5 and 6).

Somatosensory-specific neural activity (4 ± 2 ICs, contributing to both nociceptive and non-nociceptive somatosensory ERPs) explained 25 ± 21% of the LEP and 34 ± 16% of the SEP (Fig. 5). This activity contributed mainly to the early part of both ERP waveforms (Fig. 6). It appeared as a negative wave (LEP: 189 ± 28 ms; SEP: 93 ± 37 ms) whose scalp topography was distributed over central and parietal regions, and maximal over the hemisphere contralateral to the stimulated side.

Nociceptive-specific somatosensory neural activity was not identified. Indeed, not a single IC was found to contribute uniquely to the LEP waveform (Fig. 3).

Non-nociceptive–specific somatosensory neural activity. A small number of ICs (2 ± 1) contributed uniquely to the non-nociceptive SEP, explaining 8 ± 12% of that waveform (Fig. 5). This activity appeared as a negative wave peaking at 133 ± 45 ms. Its scalp topography was maximal over the central parietal region contralateral to the stimulated side.

Auditory-specific neural activity (3 ± 1 ICs, explaining 32 ± 18% of the AEP; Fig. 5) appeared as a negative wave (peaking at 101 ± 8 ms) whose scalp topography was symmetrically distributed over central, frontal, and temporal regions (Fig. 6). Similarly to somatosensory specific activities, the contribution of auditory-specific activity was confined to the early part of the AEP waveform.

Visual-specific neural activity (2 ± 1 ICs, explaining 36 ± 27% of the VEP; Fig. 5) appeared as a positive wave (peaking at 130 ± 32 ms) followed by a negative wave (peaking at 192 ± 59 ms). The two peaks of visual-specific activity had notably different scalp topographies (Fig. 6). The first peak was maximal over occipital areas. The second was more largely distributed over parietal, temporal, and occipital areas and clearly predominant over the hemisphere contralateral to the stimulated side.

DISCUSSION

Although laser stimuli activate nociceptive peripheral afferents selectively, our results indicate that laser-evoked EEG responses reflect neural activities equally involved in processing nociceptive and non-nociceptive sensory inputs. Indeed,

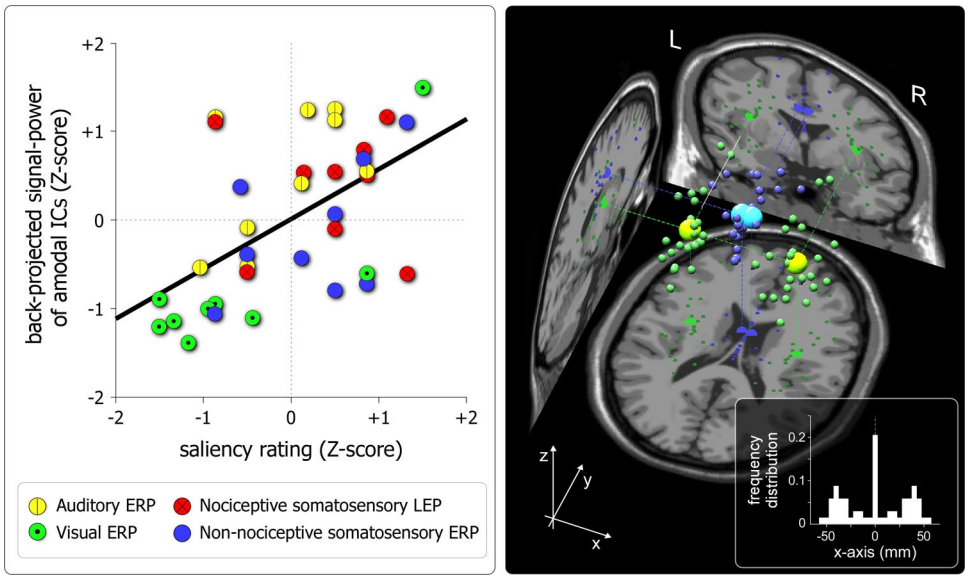

FIG. 7. Functional significance and source modeling of multimodal brain activity. *Left*: scatter plot showing the correlation between the subjective rating of stimulus saliency (shown on the *x*-axis) and the magnitude of multimodal activity (shown on the *y*-axis as the global field power averaged in the time interval ranging from 0 to +0.5 s after stimulus). Four pairs of values (expressed as z-scores to account for response variability across subjects) were obtained for each participant (1 pair of values for each of the 4 stimulus types). A significant positive correlation was observed (Pearson's $r = 0.56 \pm 0.46$, group-level average; $P = 0.009$), indicating that the magnitude of multimodal activity is determined by the saliency of the stimulus. The black line represents the average slope of the linear regressions. *Right*: sources of multimodal ICs were modeled by fitting, for each multimodal IC, a pair of symmetrical equivalent dipoles. The locations of the fitted dipoles appeared to form two clusters: a deep midline cluster (blue spheres: -20 mm $< x <$20 mm, Montreal Neurological Institute coordinates) whose center of gravity was located in the ACC, and a bilateral cluster (green spheres: $x < -20$ mm or $x >$20 mm) located in left and right operculo-insular regions (see also *bottom right inset* showing the relative frequency distribution of obtained dipole locations along the *x*-axis). The small spheres represent the fitted source location of each single IC. The larger spheres represent the center of gravity of each cluster.

LEPs were entirely explained *1*) by a major contribution of multimodal neural activities, explaining the largest part of the laser-evoked N2 and P2 waves and *2*) by a less prominent contribution of somatosensory-specific, but not nociceptive-specific, neural activities, explaining the largest part of the laser-evoked N1 wave. This finding provides, for the first time, quantitative experimental evidence in support of a possibility that had already been raised by a number of investigators (Bromm and Lorenz 1998; Carmon et al. 1976; Garcia-Larrea et al. 1997; Iannetti et al. 2008; Kunde and Treede 1993; Mouraux and Plaghki 2006)—that the activity of nociceptive-specific cortical neurons cannot be isolated using scalp LEPs.

Contribution of multimodal neural activity to LEPs

Multimodal neural activities explained 76 ± 13% of the LEP signal and were the main constituent of the entire LEP waveform, in particular the N2 wave (of which it explained 79 ± 22%) and the P2 wave (of which it explained 88 ± 17%).

What is the functional significance of this predominant multimodal activity? The observation that the magnitude of multimodal neural activity correlated with the subjective rating of stimulus saliency indicates that it at least partly reflects neural processes triggered by the occurrence of salient changes in the sensory environment, and thus that it could be related, directly or indirectly, to stimulus-triggered mechanisms of arousal and/or attentional reorientation (Ranganath and Rainer 2003). In line with this hypothesis, a number of investigators have suggested that the N2 and P2 waves of the LEP waveform reflect neural activities involved in reorienting attention toward or reacting to noxious stimuli (Garcia-Larrea 2004; Iannetti et al. 2008; Legrain et al. 2005; Mouraux and Plaghki 2006). Our results indicate that the saliency-related neural processes underlying the N2 and P2 waves are independent of the sensory modality of the eliciting stimulus and thus that they could be linked to the "multimodal cortical network for the detection of changes in the sensory environment" that was identified by Downar et al. (2000), using fMRI. These neural processes could be tightly related to those underlying the cognitive P3a wave, which has been suggested to reflect an orientation response and has been shown to contribute to both the late part of the LEP response (Legrain et al. 2002, 2005) and other vertex potentials (Friedman et al. 2001). In addition, because the intensity of a sensory stimulus is an important determinant of its saliency, our finding indicates that the positive relationship between LEP magnitude and intensity of pain (Arendt-Nielsen 1994; Beydoun et al. 1993; Bromm and Treede 1991; Garcia-Larrea et al. 1997; Iannetti et al. 2005; Kakigi et al. 1989), which has been repeatedly interpreted as evidence that LEPs reflect neural activities encoding the intensity of noxious stimuli, can be entirely explained by a modulation of the magnitude of saliency-related multimodal responses. In support of this view, we have recently shown that modulating the saliency of a nociceptive stimulus without changing its intensity (by changing the novelty of the stimulus, another important determinant of its saliency) disrupts the positive relationship between the magnitude of LEPs and the magnitude of pain perception (Iannetti et al. 2008), a finding expanding previous reports of dissociations between LEP magnitude and pain (Dillmann et al. 2000; Treede et al. 2003).

Multichannel LEP responses are usually modeled by a combination of medial cingulate sources (thought to reflect multimodal brain activity) and lateral opercular sources (thought to

reflect, at least in part, nociceptive-specific brain activity), thus leading to the dualistic view that LEPs reflect both nociceptive-specific and multimodal activities (Garcia-Larrea et al. 2003). Here, by showing that multimodal activities are modeled by sources located not only in medial, but also in lateral brain structures (Fig. 7, *right*), we suggest that the experimental evidence supporting this dualistic view does not hold. In other words, our results challenge the notion that LEP sources hypothesized to originate from the operculum may be considered as primarily nociceptive specific or even as primarily somatosensory specific. This is supported by evidence from single-cell recordings performed in rodents (Brett-Green et al. 2004; Menzel and Barth 2005; Rodgers et al. 2008; Wallace et al. 2004), showing that all these regions are at least partly involved in multimodal sensory integration (i.e., the integration of sensory inputs across multiple sensory modalities). Most importantly, single-cell recordings performed in humans and in nonhuman primates have shown that, in these regions, neurons responding to nociceptive stimuli may also respond to other kinds of salient sensory stimuli (e.g., a menacing visual stimulus; Dong et al. 1994; Hutchison et al. 1999; Kenshalo and Douglass 1995), thus suggesting that neurons identified as nociceptive-specific (because they responded to nociceptive somatosensory stimuli but not to non-nociceptive somatosensory stimuli) could in fact be multimodal, and their activity could be largely determined by the saliency of the stimulus. This hypothesis would agree with the results of a number of human EEG and fMRI studies, showing that non-nociceptive somatosensory stimuli also elicit activity in these regions and that the magnitude of this activity is largely determined by the saliency of the eliciting stimulus (Burton et al. 1999; Chen et al. 2008; Menon et al. 1997; Ranganath and Rainer 2003).

What could be the anatomical connections underlying the generation of these multimodal brain responses? In the classical hierarchical view of sensory processing, multimodal cortical activity reflects high-level sensory or cognitive processes that occur only after sensory signals have undergone extensive processing within modality-specific cortices. However, another possibility is that multimodal cortical activity is the consequence of multimodal convergence that has already occurred at the subcortical level (reviewed in Schroeder and Foxe 2005). Indeed, thalamo-cortical projections that are already multimodal could originate either from aspecific laminar thalamic nuclei or from the calbindin-positive matrix of thalamic cells (Jones 1998b). This "thalamic matrix," which ignores the classical nuclear organization of the thalamus, receives diffuse sensory input and projects to virtually all cortical areas, has been proposed to constitute a diffuse multimodal system that plays an important role for generating conscious perception (by binding multiple aspects of sensory experience), detecting changes in the sensory environment, and triggering arousal reactions. The hypothesis that multimodal cortical activity relates to such a system would agree with the early proposals that vertex potentials mainly reflect a nonspecific cortical response triggered by diffuse thalamo-cortical projections (Davis et al. 1966), as well as with the later description of a multimodal contribution to vertex potentials elicited by auditory, somatosensory, and visual stimuli (reviewed in Naatanen and Picton 1987).

An important implication of our finding is that great care should be taken when interpreting observed modulations of the magnitude of vertex potentials. Indeed, although these modulations are often interpreted as evidence for a specific effect on somatosensory, auditory, or visual processing, in many cases, they can actually be explained entirely by an unaccounted modulation of multimodal activity resulting from an unaccounted change in stimulus saliency. For example, the observation of a reduction of LEP magnitude by concomitant tactile stimulation (Kakigi and Shibasaki 1992; Towell and Boyd 1993) has been interpreted as evidence consistent with the gating of nociceptive input at spinal level (Melzack and Wall 1965), and a consequent "functional decrease in the Aδ pathway." However, because the saliency of a sensory stimulus is partly determined by the amount of masking background noise (Franklin et al. 2007; Kayser et al. 2005), such results can be alternatively explained by a nonspecific reduction in the saliency of the laser stimulus when delivered concomitantly with tonic non-nociceptive somatosensory stimulation.

Similarly, a number of recent studies using EEG and fMRI have shown that experiencing empathy for pain elicits neural activity similar to that elicited by nociceptive stimuli, a finding interpreted as evidence that empathy for pain is generated through a mirror activation of the "pain matrix" (Singer et al. 2004; Valeriani et al. 2008). Our results suggest an alternative interpretation. Because experiencing empathy for pain constitutes a salient sensory event, it is likely to trigger multimodal brain responses similar to the multimodal brain responses elicited by salient nociceptive stimuli.

Contribution of somatosensory-specific, but not nociceptive-specific, activity to LEPs

The small fraction of the LEP waveform that was not explained by multimodal neural activity was almost entirely explained by somatosensory-specific, but not nociceptive-specific, neural activity (i.e., neural activity triggered by both nociceptive and non-nociceptive somatosensory stimuli). This somatosensory-specific activity was maximal over the central-parietal region contralateral to the stimulated hand (Fig. 6) and contributed mainly to the early part of the LEP time course, coinciding with the latency of the N1 wave (of which it explained 52 ± 37%) and the N2 wave (of which it explained 35 ± 29%). In contrast, nociceptive-specific neural activity (i.e., neural activity elicited uniquely by nociceptive somatosensory stimuli) did not contribute to the LEP waveform (Figs. 3 and 5).

How can these findings be reconciled with the experimental evidence indicating the existence of nociceptive-specific neurons in SI, SII, the ACC, and the insula? A first possibility is that the activity of nociceptive-specific cortical neurons in these areas does not summate into a measurable scalp EEG response. Indeed, a finding common to all reports of single-cell animal recordings is that truly nociceptive-specific cortical neurons (i.e., neurons responding uniquely to nociceptive stimulation) are extremely sparse (Kenshalo and Isensee 1983; Kenshalo et al. 2000; Robinson and Burton 1980; Sikes and Vogt 1992; Whitsel et al. 1969; Yamamura et al. 1996), and that the majority of neurons responding to nociceptive stimuli also respond to non-nociceptive somatosensory stimuli and, in some cases, even to non-somatosensory stimuli. Furthermore, following nociceptive stimulation, the firing rate of nociceptive-specific neurons is usually far lower than the firing rate of

these wide dynamic-range neurons (Kenshalo and Isensee 1983; Kenshalo et al. 2000). Therefore because scalp EEG only detects neural activity arising from large and synchronously active neuronal populations (Nunez and Srinivasan 2006), it is highly likely that the postsynaptic activity generated by the sparse population of nociceptive-specific neurons does not summate into a measurable scalp EEG response, whereas the postsynaptic activity of the comparatively higher number of wide-dynamic range neurons does summate into a measurable scalp EEG response. For this reason we believe that postsynaptic activity in wide dynamic range neurons underlies the somatosensory-specific fraction of the LEP response (Fig. 3). Notably, despite being non nociceptive specific, this activity could contribute to the perception of pain. A second possibility is that the postsynaptic activity of nociceptive-specific neurons does translate into a measurable scalp EEG response but that this response is spatially indistinguishable from the response generated by non-nociceptive-specific somatosensory neurons. In support of this alternative possibility, studies have shown that, in SI, nociceptive-specific and non-nociceptive-specific somatosensory neurons are intermingled and have very similar receptive fields (Kenshalo and Isensee 1983). Furthermore, direct electrical stimulation of the posterior insula in humans may elicit either painful or nonpainful somesthetic sensations, thus suggesting that "painful and nonpainful somesthetic representations in the human insula overlap" (Ostrowsky et al. 2002). Therefore should nociceptive-specific neurons contribute to the measured EEG response, their contribution would probably be spatially indistinguishable from the contribution of neighboring neurons responding to non-nociceptive somatosensory stimuli applied to the same body location.

Contribution of touch-specific activity to non-nociceptive SEPs

A small fraction (8 ± 12%) of the ERP waveform elicited by non-nociceptive somatosensory stimuli was shown to reflect neural activity specific for the processing of tactile stimuli (i.e., neural activity elicited by non-nociceptive somatosensory stimulation but not by nociceptive somatosensory stimulation), and, given its central-parietal distribution maximal contralateral to the stimulated side, possibly originating from the contralateral SI. This interpretation would agree with the results of intracranial recordings in humans and optical imaging studies in monkeys showing that non-nociceptive somatosensory stimuli, but not nociceptive somatosensory stimuli, elicit consistent responses within area 3b of the primary somatosensory cortex (Tommerdahl et al. 1998; Valeriani et al. 2004).

Conclusion

By showing that LEPs can be entirely explained by a combination of multimodal and somatosensory-specific (but not nociceptive-specific) neural activities, our results provide compelling evidence that the activity of nociceptive-specific cortical neurons cannot be explored using conventional analysis of scalp LEPs.

These results further question the appropriateness of relying on LEPs to build models of the cortical processes underlying nociception (Iannetti et al. 2008).

Notably, our results do not question the usefulness of LEPs to document dysfunctions of nociceptive afferent pathways or to explore the effect of a given experimental factor on the transmission and processing of nociceptive input. Indeed, even if LEPs reflect neuronal activities that are entirely unspecific for the nociceptive system, their generation still relies on the functional state of the nociceptive system, both at peripheral and central levels. Consequently, when carefully used, LEPs can still be reliably used to obtain a readout—albeit indirect—of the function of the afferent nociceptive system.

ACKNOWLEDGMENTS

We are grateful to P. Neri, A. C. Nobre, L. Plaghki, B. Rossion, and the members of the GAMFI Centre for insightful comments. We also thank C. Beckmann and S. Makni for sharing knowledge of probabilistic ICA.

GRANTS

A. Mouraux is a Marie-Curie postdoctoral Research Fellow and a Chargé de recherches of the Belgian National Fund for Scientific Research. G. D. Iannetti is University Research Fellow of The Royal Society.

REFERENCES

Arendt-Nielsen L. Characteristics, detection, and modulation of laser-evoked vertex potentials. *Acta Anaesthesiol Scand Suppl* 101: 7–44, 1994.

Beckmann CF, Smith SA. Probabilistic independent component analysis for functional magnetic resonance imaging. *IEEE Trans Med Imaging* 23: 137–152, 2004.

Bell AJ, Sejnowski TJ. An information-maximization approach to blind separation and blind deconvolution. *Neural Comput* 7: 1129–1159, 1995.

Beydoun A, Morrow TJ, Shen JF, Casey KL. Variability of laser-evoked potentials: attention, arousal and lateralized differences. *Electroencephalogr Clin Neurophysiol* 88: 173–181, 1993.

Boly M, Faymonville ME, Schnakers C, Peigneux P, Lambermont B, Phillips C, Lancellotti P, Luxen A, Lamy M, Moonen G, Maquet P, Laureys S. Perception of pain in the minimally conscious state with PET activation: an observational study. *Lancet Neurol* 7: 1013–1020, 2008.

Brett-Green B, Paulsen M, Staba RJ, Fifkova E, Barth DS. Two distinct regions of secondary somatosensory cortex in the rat: topographical organization and multisensory responses. *J Neurophysiol* 91: 1327–1336, 2004.

Bromm B, Lorenz J. Neurophysiological evaluation of pain. *Electroencephalogr Clin Neurophysiol* 107: 227–253, 1998.

Bromm B, Treede RD. Nerve fibre discharges, cerebral potentials and sensations induced by CO2 laser stimulation. *Hum Neurobiol* 3: 33–40, 1984.

Bromm B, Treede RD. Human cerebral potentials evoked by CO2 laser stimuli causing pain. *Exp Brain Res* 67: 153–162, 1987.

Bromm B, Treede RD. Laser-evoked cerebral potentials in the assessment of cutaneous pain sensitivity in normal subjects and patients. *Rev Neurol (Paris)* 147: 625–643, 1991.

Brooks J, Tracey I. From nociception to pain perception: imaging the spinal and supraspinal pathways. *J Anat* 207: 19–33, 2005.

Burgess PR, Perl ER. Myelinated afferent fibres responding specifically to noxious stimulation of the skin. *J Physiol* 190: 541–562, 1967.

Burton H, Abend NS, MacLeod AM, Sinclair RJ, Snyder AZ, Raichle ME. Tactile attention tasks enhance activation in somatosensory regions of parietal cortex: a positron emission tomography study. *Cereb Cortex* 9: 662–674, 1999.

Bushnell MC, Apkarian AV.Representation of pain in the brain. In: *Textbook of Pain* (5th ed.), edited by McMahon S, Koltzenburg M. Churchill Livingstone, 2005, p. 267–289.

Carmon A, Mor J, Goldberg J. Evoked cerebral responses to noxious thermal stimuli in humans. *Exp Brain Res* 25: 103–107, 1976.

Chen TL, Babiloni C, Ferretti A, Perrucci MG, Romani GL, Rossini PM, Tartaro A, Del Gratta C. Human secondary somatosensory cortex is involved in the processing of somatosensory rare stimuli: an fMRI study. *Neuroimage* 40: 1765–1771, 2008.

Cheng Y, Lin CP, Liu HL, Hsu YY, Lim KE, Hung D, Decety J. Expertise modulates the perception of pain in others. *Curr Biol* 17: 1708–1713, 2007.

Coghill RC, Sang CN, Maisog JM, Iadarola MJ. Pain intensity processing within the human brain: a bilateral, distributed mechanism. *J Neurophysiol* 82: 1934–1943, 1999.

Costantini M, Galati G, Romani GL, Aglioti SM. Empathic neural reactivity to noxious stimuli delivered to body parts and non-corporeal objects. *Eur J Neurosci* 28: 1222–1230, 2008.

Davis H, Mast T, Yoshie N, Zerlin S. The slow response of the human cortex to auditory stimuli: recovery process. *Electroencephalogr Clin Neurophysiol* 21: 105–113, 1966.

Decety J, Michalska KJ, Akitsuki Y, Lahey BB. Atypical empathic responses in adolescents with aggressive conduct disorder: a functional MRI investigation. *Biol Psychol* 80: 203–211, 2008.

Delorme A, Makeig S. EEGLAB: an open source toolbox for analysis of single-trial EEG dynamics including independent component analysis. *J Neurosci Methods* 134: 9–21, 2004.

Derbyshire SW, Jones AK, Gyulai F, Clark S, Townsend D, Firestone LL. Pain processing during three levels of noxious stimulation produces differential patterns of central activity. *Pain* 73: 431–445, 1997.

Dillmann J, Miltner WH, Weiss T. The influence of semantic priming on event-related potentials to painful laser-heat stimuli in humans. *Neurosci Lett* 284: 53–56, 2000.

Dong WK, Chudler EH, Sugiyama K, Roberts VJ, Hayashi T. Somatosensory, multisensory, and task-related neurons in cortical area 7b (PF) of unanesthetized monkeys. *J Neurophysiol* 72: 542–564, 1994.

Downar J, Crawley AP, Mikulis DJ, Davis KD. A multimodal cortical network for the detection of changes in the sensory environment. *Nat Neurosci* 3: 277–283, 2000.

Ducreux D, Attal N, Parker F, Bouhassira D. Mechanisms of central neuropathic pain: a combined psychophysical and fMRI study in syringomyelia. *Brain* 129: 963–976, 2006.

Franklin JC, Moretti NA, Blumenthal TD. Impact of stimulus signal-to-noise ratio on prepulse inhibition of acoustic startle. *Psychophysiology* 44: 339–342, 2007.

Friedman D, Cycowicz YM, Gaeta H. The novelty P3: an event-related brain potential (ERP) sign of the brain's evaluation of novelty. *Neurosci Biobehav Rev* 25: 355–373, 2001.

Frot M, Mauguiere F. Dual representation of pain in the operculo-insular cortex in humans. *Brain* 126: 438–450, 2003.

Frot M, Mauguiere F, Magnin M, Garcia-Larrea L. Parallel processing of nociceptive A-delta inputs in SII and midcingulate cortex in humans. *J Neurosci* 28: 944–952, 2008.

Frot M, Rambaud L, Guenot M, Mauguiere F. Intracortical recordings of early pain-related CO2-laser evoked potentials in the human second somatosensory (SII) area. *Clin Neurophysiol* 110: 133–145, 1999.

Fuchs M, Kastner J, Wagner M, Hawes S, Ebersole JS. A standardized boundary element method volume conductor model. *Clin Neurophysiol* 113: 702–712, 2002.

Garcia-Larrea L. Somatosensory volleys and cortical evoked potentials: 'first come, first served'? *Pain* 112: 5–7, 2004.

Garcia-Larrea L, Frot M, Valeriani M. Brain generators of laser-evoked potentials: from dipoles to functional significance. *Neurophysiol Clin* 33: 279–292, 2003.

Garcia-Larrea L, Lukaszewicz AC, Mauguiere F. Somatosensory responses during selective spatial attention: the N120-to-N140 transition. *Psychophysiology* 32: 526–537, 1995.

Garcia-Larrea L, Peyron R, Laurent B, Mauguiere F. Association and dissociation between laser-evoked potentials and pain perception. *Neuroreport* 8: 3785–3789, 1997.

Goff GD, Matsumiya Y, Allison T, Goff WR. The scalp topography of human somatosensory and auditory evoked potentials. *Electroencephalogr Clin Neurophysiol* 42: 57–76, 1977.

Hofbauer RK, Rainville P, Duncan GH, Bushnell MC. Cortical representation of the sensory dimension of pain. *J Neurophysiol* 86: 402–411, 2001.

Hutchison WD, Davis KD, Lozano AM, Tasker RR, Dostrovsky JO. Pain-related neurons in the human cingulate cortex. *Nat Neurosci* 2: 403–405, 1999.

Iannetti GD, Hughes NP, Lee MC, Mouraux A. Determinants of laser-evoked EEG responses: pain perception or stimulus saliency?. *J Neurophysiol* 100: 815–828, 2008.

Iannetti GD, Zambreanu L, Cruccu G, Tracey I. Operculoinsular cortex encodes pain intensity at the earliest stages of cortical processing as indicated by amplitude of laser-evoked potentials in humans. *Neuroscience* 131: 199–208, 2005.

Iannetti GD, Zambreanu L, Tracey I. Similar nociceptive afferents mediate psychophysical and electrophysiological responses to heat stimulation of glabrous and hairy skin in humans. *J Physiol* 577: 235–248, 2006.

Ingvar M. Pain and functional imaging. *Philos Trans R Soc Lond B Biol Sci* 354: 1347–1358, 1999.

Inui K, Tran TD, Qiu Y, Wang X, Hoshiyama M, Kakigi R. A comparative magnetoencephalographic study of cortical activations evoked by noxious and innocuous somatosensory stimulations. *Neuroscience* 120: 235–248, 2003.

Jones A. The pain matrix and neuropathic pain. *Brain* 121: 783–784, 1998a.

Jones EG. Viewpoint: the core and matrix of thalamic organization. *Neuroscience* 85: 331–345, 1998b.

Jung TP, Makeig S, Humphries C, Lee TW, McKeown MJ, Iragui V, Sejnowski TJ. Removing electroencephalographic artifacts by blind source separation. *Psychophysiology* 37: 163–178, 2000.

Kakigi R, Inui K, Tamura Y. Electrophysiological studies on human pain perception. *Clin Neurophysiol* 116: 743–763, 2005.

Kakigi R, Shibasaki H. Mechanisms of pain relief by vibration and movement. *J Neurol Neurosurg Psychiatry* 55: 282–286, 1992.

Kakigi R, Shibasaki H, Ikeda A. Pain-related somatosensory evoked potentials following CO2 laser stimulation in man. *Electroencephalogr Clin Neurophysiol* 74: 139–146, 1989.

Kayser C, Petkov CI, Lippert M, Logothetis NK. Mechanisms for allocating auditory attention: an auditory saliency map. *Curr Biol* 15: 1943–1947, 2005.

Kenshalo DR, Douglass DK.The role of the cerebral cortex in the experience of pain. In: *Pain and the Brain: From Nociception to Cognition*, edited by Bromm B, Desmedt JE. New York: Raven Press, 1995, p. 21–34.

Kenshalo DR, Iwata K, Sholas M, Thomas DA. Response properties and organization of nociceptive neurons in area 1 of monkey primary somatosensory cortex. *J Neurophysiol* 84: 719–729, 2000.

Kenshalo DR Jr, Isensee O. Responses of primate SI cortical neurons to noxious stimuli. *J Neurophysiol* 50: 1479–1496, 1983.

Kunde V, Treede RD. Topography of middle-latency somatosensory evoked potentials following painful laser stimuli and non-painful electrical stimuli. *Electroencephalogr Clin Neurophysiol* 88: 280–289, 1993.

Legrain V, Bruyer R, Guerit JM, Plaghki L. Nociceptive processing in the human brain of infrequent task-relevant and task-irrelevant noxious stimuli. A study with event-related potentials evoked by CO2 laser radiant heat stimuli. *Pain* 103: 237–248, 2003.

Legrain V, Bruyer R, Guerit JM, Plaghki L. Involuntary orientation of attention to unattended deviant nociceptive stimuli is modulated by concomitant visual task difficulty. Evidence from laser evoked potentials. *Clin Neurophysiol* 116: 2165–2174, 2005.

Legrain V, Guerit JM, Bruyer R, Plaghki L. Attentional modulation of the nociceptive processing into the human brain: selective spatial attention, probability of stimulus occurrence, and target detection effects on laser evoked potentials. *Pain* 99: 21–39, 2002.

Lehmann D, Skrandies W. Reference-free identification of components of checkerboard-evoked multichannel potential fields. *Electroencephalogr Clin Neurophysiol* 48: 609–621, 1980.

Lenz FA, Rios M, Chau D, Krauss GL, Zirh TA, Lesser RP. Painful stimuli evoke potentials recorded from the parasylvian cortex in humans. *J Neurophysiol* 80: 2077–2088, 1998a.

Lenz FA, Rios M, Zirh A, Chau D, Krauss G, Lesser RP. Painful stimuli evoke potentials recorded over the human anterior cingulate gyrus. *J Neurophysiol* 79: 2231–2234, 1998b.

Lorenz J, Garcia-Larrea L. Contribution of attentional and cognitive factors to laser evoked brain potentials. *Neurophysiol Clin* 33: 293–301, 2003.

Maihofner C, Ringler R, Herrndobler F, Koppert W. Brain imaging of analgesic and antihyperalgesic effects of cyclooxygenase inhibition in an experimental human pain model: a functional MRI study. *Eur J Neurosci* 26: 1344–1356, 2007.

Makeig S, Jung TP, Bell AJ, Ghahremani D, Sejnowski TJ. Blind separation of auditory event-related brain responses into independent components. *Proc Natl Acad Sci USA* 94: 10979–10984, 1997.

Makeig S, Westerfield M, Townsend J, Jung TP, Courchesne E, Sejnowski TJ. Functionally independent components of early event-related potentials in a visual spatial attention task. *Philos Trans R Soc Lond B Biol Sci* 354: 1135–1144, 1999.

Melzack R, Wall PD. Pain mechanisms: a new theory. *Science* 150: 971–979, 1965.

Menon V, Ford JM, Lim KO, Glover GH, Pfefferbaum A. Combined event-related fMRI and EEG evidence for temporal-parietal cortex activation during target detection. *Neuroreport* 8: 3029–3037, 1997.

Menzel RR, Barth DS. Multisensory and secondary somatosensory cortex in the rat. *Cereb Cortex* 15: 1690–1696, 2005.

Moisset X, Bouhassira D. Brain imaging of neuropathic pain. *Neuroimage* 37: S80–S88, 2007.

Mouraux A, Iannetti GD. Across-trial averaging of event-related EEG responses and beyond. *Magn Reson Imaging* 26: 1041–1054, 2008.

Mouraux A, Plaghki L. Are the processes reflected by late and ultra-late laser evoked potentials specific of nociception?. *Clin Neurophysiol* 59: 197–204, 2006.

Naatanen R, Picton T. The N1 wave of the human electric and magnetic response to sound: a review and an analysis of the component structure. *Psychophysiology* 24: 375–425, 1987.

Nunez PL, Srinivasan R. *Electric Fields of the Brain. The Neurophysics of EEG.* New York: Oxford, 2006, p. 640.

Ohara S, Crone NE, Weiss N, Treede RD, Lenz FA. Amplitudes of laser evoked potential recorded from primary somatosensory, parasylvian and medial frontal cortex are graded with stimulus intensity. *Pain* 110: 318–328, 2004.

Ostrowsky K, Magnin M, Ryvlin P, Isnard J, Guenot M, Mauguiere F. Representation of pain and somatic sensation in the human insula: a study of responses to direct electrical cortical stimulation. *Cereb Cortex* 12: 376–385, 2002.

Peyron R, Frot M, Schneider F, Garcia-Larrea L, Mertens P, Barral FG, Sindou M, Laurent B, Mauguiere F. Role of operculoinsular cortices in human pain processing: converging evidence from PET, fMRI, dipole modeling, and intracerebral recordings of evoked potentials. *Neuroimage* 17: 1336–1346, 2002.

Peyron R, Laurent B, Garcia-Larrea L. Functional imaging of brain responses to pain. A review and meta-analysis. *Neurophysiol Clin* 30: 263–288, 2000.

Picton TW, Alain C, Woods DL, John MS, Scherg M, Valdes-Sosa P, Bosch-Bayard J, Trujillo NJ. Intracerebral sources of human auditory-evoked potentials. *Audiol Neurootol* 4: 64–79, 1999.

Porro CA. Functional imaging and pain: behavior, perception, and modulation. *Neuroscientist* 9: 354–369, 2003.

Rainville P, Duncan GH, Price DD, Carrier B, Bushnell MC. Pain affect encoded in human anterior cingulate but not somatosensory cortex. *Science* 277: 968–971, 1997.

Rajan JJ, Rayner PJW. Model order selection for the singular value decomposition and the discrete Karhunen-Loeve transform using a Bayesian approach. *Vision Image Signal Processing IEEE Proc* 144: 116–123, 1997.

Ranganath C, Rainer G. Neural mechanisms for detecting and remembering novel events. *Nat Rev Neurosci* 4: 193–202, 2003.

Robinson CJ, Burton H. Somatotopographic organization in the second somatosensory area of M. fascicularis. *J Comp Neurol* 192: 43–67, 1980.

Rodgers KM, Benison AM, Klein A, Barth DS. Auditory, somatosensory, and multisensory insular cortex in the rat. *Cereb Cortex* 18: 2941–2951, 2008.

Schlereth T, Baumgartner U, Magerl W, Stoeter P, Treede RD. Left-hemisphere dominance in early nociceptive processing in the human parasylvian cortex. *Neuroimage* 20: 441–454, 2003.

Schroeder CE, Foxe J. Multisensory contributions to low-level, 'unisensory' processing. *Curr Opin Neurobiol* 15: 454–458, 2005.

Sikes RW, Vogt BA. Nociceptive neurons in area 24 of rabbit cingulate cortex. *J Neurophysiol* 68: 1720–1732, 1992.

Singer T, Seymour B, O'Doherty J, Kaube H, Dolan RJ, Frith CD. Empathy for pain involves the affective but not sensory components of pain. *Science* 303: 1157–1162, 2004.

Stern J, Jeanmonod D, Sarnthein J. Persistent EEG overactivation in the cortical pain matrix of neurogenic pain patients. *Neuroimage* 31: 721–731, 2006.

Stowell H. Event related brain potentials and human pain: a first objective overview. *Int J Psychophysiol* 1: 137–151, 1984.

Tommerdahl M, Delemos KA, Favorov OV, Metz CB, Vierck CJ Jr, Whitsel BL. Response of anterior parietal cortex to different modes of same-site skin stimulation. *J Neurophysiol* 80: 3272–3283, 1998.

Towell AD, Boyd SG. Sensory and cognitive components of the CO2 laser evoked cerebral potential. *Electroencephalogr Clin Neurophysiol* 88: 237–239, 1993.

Treede RD, Kenshalo DR, Gracely RH, Jones AK. The cortical representation of pain. *Pain* 79: 105–111, 1999.

Treede RD, Kief S, Holzer T, Bromm B. Late somatosensory evoked cerebral potentials in response to cutaneous heat stimuli. *Electroencephalogr Clin Neurophysiol* 70: 429–441, 1988.

Treede RD, Lorenz J, Baumgartner U. Clinical usefulness of laser-evoked potentials. *Neurophysiol Clin* 33: 303–314, 2003.

Treede RD, Meyer RA, Raja SN, Campbell JN. Evidence for two different heat transduction mechanisms in nociceptive primary afferents innervating monkey skin. *J Physiol* 483: 747–758, 1995.

Valeriani M, Barba C, Le Pera D, Restuccia D, Colicchio G, Tonali P, Gagliardo O, Treede RD. Different neuronal contribution to N20 somatosensory evoked potential and to CO2 laser evoked potentials: an intracerebral recording study. *Clin Neurophysiol* 115: 211–216, 2004.

Valeriani M, Betti V, Le Pera D, De Armas L, Miliucci R, Restuccia D, Avenanti A, Aglioti SM. Seeing the pain of others while being in pain: a laser-evoked potentials study. *Neuroimage* 40: 1419–1428, 2008.

Vogel EK, Luck SJ. The visual N1 component as an index of a discrimination process. *Psychophysiology* 37: 190–203, 2000.

Wallace MT, Ramachandran R, Stein BE. A revised view of sensory cortical parcellation. *Proc Natl Acad Sci USA* 101: 2167–2172, 2004.

Whitsel BL, Petrucelli LM, Werner G. Symmetry and connectivity in the map of the body surface in somatosensory area II of primates. *J Neurophysiol* 32: 170–183, 1969.

Whyte J. Clinical implications of the integrity of the pain matrix. *Lancet Neurol* 7: 979–980, 2008.

Woody C. Characterization of an adaptive filter for the analysis of variable latency neuroelectric signals. *Med Biol Eng* 5: 539–553, 1967.

Yamamura H, Iwata K, Tsuboi Y, Toda K, Kitajima K, Shimizu N, Nomura H, Hibiya J, Fujita S, Sumino R. Morphological and electrophysiological properties of ACCx nociceptive neurons in rats. *Brain Res* 735: 83–92, 1996.

Volume 101, June 2009

Mouraux A, Iannetti GD. Nociceptive Laser-Evoked Brain Potentials Do Not Reflect Nociceptive-Specific Neural Activity. *J Neurophysiol* 101: 3258–3269, 2009; doi:10.1152/jn.91181.2008; http://jn.physiology.org/cgi/content/full/101/6/3258.

During production, Figs. 4 and 6 were switched. The final published article incorrectly shows Fig. 6 with the legend to Fig. 4 and Fig. 4 with the legend to Fig. 6. The two figures are correctly numbered and given with their legends here.

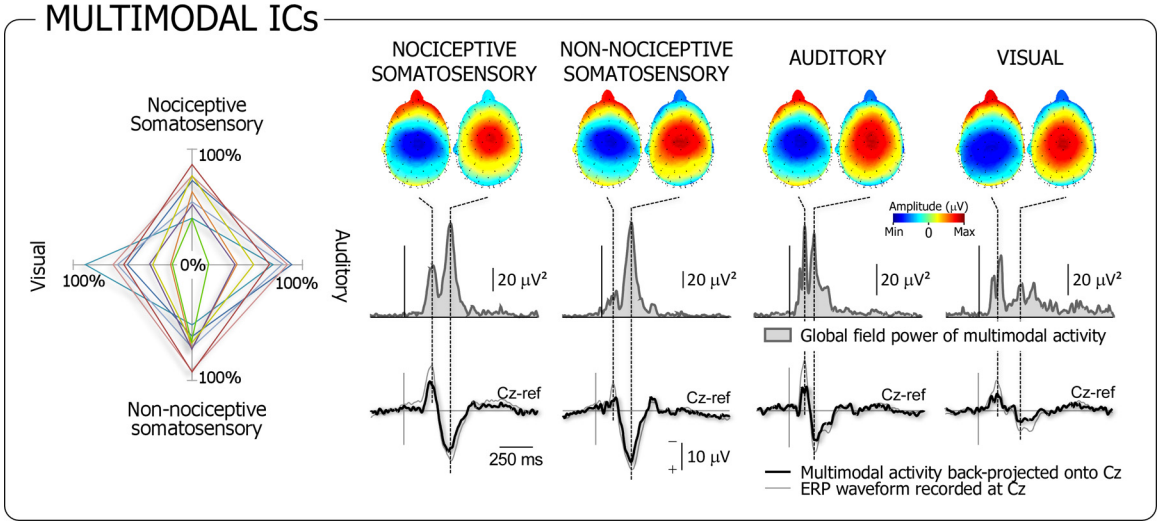

FIG. 4. Contribution of multimodal brain activity to sensory ERPs. PICA was used to break down ERPs of each participant into a set of multimodal and modality-specific ICs. *Left*: the spider chart shows the respective contribution of multimodal activity (expressed as the percentage of explained ERP variance) to the four sensory ERPs (represented on the four axes). Each colored line represents a single participant. Note how this multimodal activity contributes significantly to the four sensory ERPs in each participant. *Right*: the time course of multimodal activity, backprojected on the scalp and expressed as global field power (μV^2), is shown in the middle graphs (group average). Whatever the sensory modality of the eliciting stimulus, multimodal activity forms two peaks, whose scalp topographies are maximal at the vertex (top scalp maps). Note (bottom waveforms) how multimodal activity (thick line) explains the greater part of the ERP recorded at the scalp vertex (thin gray line).

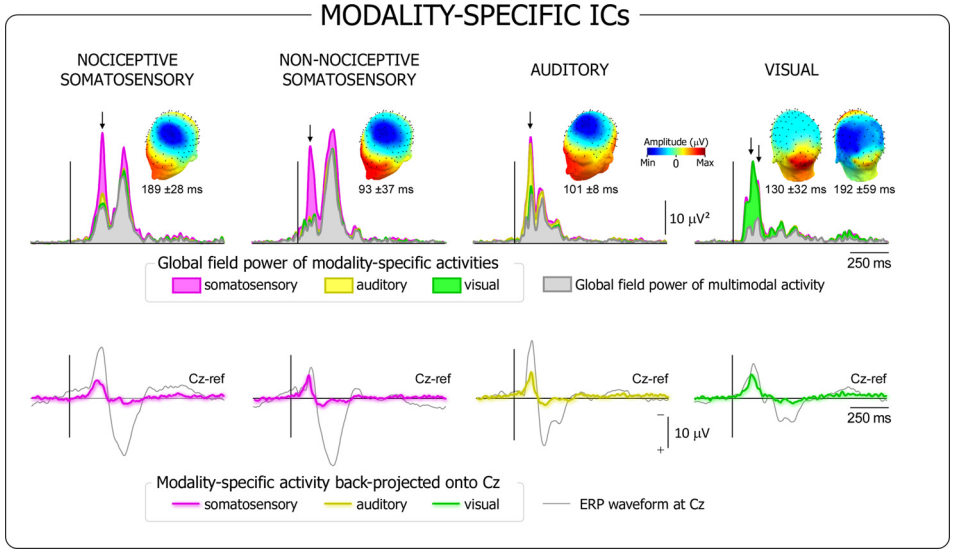

FIG. 6. Time course and scalp topography of modality-specific brain activity contributing to sensory ERPs. *Top row*: the group average time courses of multimodal (in gray) and modality-specific (in color) activities are shown in the cumulative stacked waveforms, backprojected on the scalp and expressed as the signal global field power (μV^2). *Bottom row*: average contribution of modality-specific brain activities (colored waveforms) to the ERP recorded from electrode Cz (thin gray waveform). Note how the contribution of somatosensory, auditory, and visual-specific activity is largely confined to the early part of the ERP time course. The scalp maps show the scalp topography of the main peaks of modality-specific brain activity. Somatosensory-specific activity appeared as a negative peak distributed over central and parietal regions, and maximal over the hemisphere contralateral to the stimulated side. Auditory-specific activity appeared as negative peak symmetrically distributed over central, frontal, and temporal regions. Visual-specific activity appeared as a positive peak followed by a negative peak, each peak showing a distinct scalp topography. The 1st peak of visual-specific activity was maximal over occipital areas. The 2nd was more largely distributed over parietal, temporal, and occipital areas and was maximal over the hemisphere contralateral to the stimulated side.